Available online at www.sciencedirect.com
SCIENCE DIRECT
Biochemical Pharmacology 70 (2005) 37–46
Biochemical Pharmacology
www.elsevier.com/locate/biochempharm

Identification of a drug target motif: An anti-tumor drug NK109 interacts with a PNxxxxP

Kengo Morohashi [a], Ayako Yoshino [b], Atsushi Yoshimori [a], Seiichi Saito [c], Seiichi Tanuma [a], Kengo Sakaguchi [a,b], Fumio Sugawara [a,b,*]

[a] *Genome and Drug Research Center, Tokyo University of Science, 2641 Yamazaki, Noda-shi, Chiba 278-8510, Japan*
[b] *Department of Applied Biological Science, Tokyo University of Science, 2641 Yamazaki Noda, Chiba 278-8510, Japan*
[c] *Medicinal Chemistry Group, Drug Research Department, Nippon Kayaku Co., Ltd, 31-12 Shimo-3-chome, Kita-ku, Tokyo 115-8588, Japan*

Received 7 February 2005; accepted 18 March 2005

Abstract

The synthetic compound NK109 shows anti-tumor effects against a number of human cancer cell lines. The mechanism of action is thought to involve the inhibition of DNA topoisomerase II. However, NK109 also exhibits potent anti-tumor activities against doxorubicin-, cisplatin- and etoposide-resistant human cell lines. This paper describes target validation of NK109 using biotinylated NK109 and a T7 phage library screening procedure. Phage particles displaying an affinity for NK109 were isolated and the DNA sequence determined. The amino acid sequences of selected peptides, and the results of mutation experiments by alanine scanning, confirmed that the binding target motif of NK109 is PNxxxxP. In silico analysis of the interaction between NK109 and the peptide, by docking simulation and molecular dynamics, supported this conclusion. The PNxxxxP motif exists in the C2 domain of protein kinase Cα. NK109 was confirmed to bind the C2 domain from surface plasmon resonance analysis. Furthermore, NK109 moderately inhibited protein kinase C activity in vitro. Our results show that the anti-tumor activity of NK109 stems from interactions with multiple protein targets.
© 2005 Elsevier Inc. All rights reserved.

Keywords: NK109; Benzo[*c*]phenanthridine; Anti-cancer; Phage display; Molecular dynamics; Drug binding motif

1. Introduction

NK109, 7-hydroxy-8-methoxy-5-methyl-2,3-methylenedioxybenzo[*c*]phenanthridium (**1**) is a synthetic derivative of the benzo[*c*]phenanthridine family and has anti-tumor activities against several murine cell lines including P 388, L1210 leukemia, colon 26 and B16 human melanoma as well as drug-resistant human tumor cell lines [1–4]. Some derivatives of the benzo[*c*]phenanthridine family inhibit topoisomerase activity through the stabilization of the cleavable complex [5]. Besides them, chelerythrine chloride specifically inhibits protein kinase C (PKC) and induces tumor cell toxicity and growth delay [6]. NK109 inhibits topoisomerase at >100 μM in vitro. Nevertheless, NK109 exhibits potent anti-tumor activity at lower concentration (<1 μM) against human cell lines with resistance against agents, such as doxorubicin, cisplatin or etoposide [2]. These suggest that NK109 would affect various protein functions. In order to elucidate the anti-tumor activity of NK109, identification of target motif of NK109 should be required.

Phage display cloning is one of the best methods for the identification of drug binding proteins. This method has been applied successfully to determine the protein target of several small molecule drugs including paclitaxel, FK506, doxorubicin, SQMG and HBC [7–12]. Phage display also has the advantage of not only identifying the target protein but also the binding site in terms of a peptide sequence. In this study, we have used phage display screening to identify the target motif of NK109, which was then verified by alanine scanning and in silico docking analyses. Indeed the binding motif (PNxxxxP) was found in the C2 domain of PKCα, which is inhibited by NK109 in vitro.

Abbreviations: PKCα, protein kinase Cα; SPR, surface plasmon resonance

* Corresponding author. Tel.: +81 4 7124 1501; fax: +81 4 7123 9767.
E-mail address: sugawara@rs.noda.tus.ac.jp (F. Sugawara).

0006-2952/$ – see front matter © 2005 Elsevier Inc. All rights reserved.
doi:10.1016/j.bcp.2005.03.035

2. Materials and methods

2.1. Synthesis of biotinylated NK109, 7-hydroxy-8-{2-[3-(N-biotiny)aminopropionyloxy]-ethoxy}-5-methyl-2,3-methylenedioxybenzo[c]phenanthridium chloride (4)

To a solution of **1** [4] (9 mg, 0.02 mmol) dissolved in CH_2Cl_2 (20 ml) is added water (10 ml), and then water phase was adjusted to pH 9.0 with 0.1N NaOH solution. Subsequently, CH_2Cl_2 (15 ml) MeOH (1.5 ml) and water (10 ml) were added, and after shaking, the organic phase was separated. Extraction with CH_2Cl_2 was repeated several times. The organic layers were combined, dried over anhydrous Na_2SO_4, and concentrated in vacuo. The residue was chromatographed on silica gel eluting with $CHCl_3$/MeOH (5/1 v/v) to afford a desired **2** (6 mg, 75%): ESI-MS m/z 364 $(M + H)^+$. To a solution of **2** (32 mg, 0.08 mmol) in dry CH_2Cl_2 (22 ml) is added **3** (83 mg, 0.26 mmol), *N*,*N*′-dicyclohexylcarbodiimide (70.8 mg, 0.34 mmol) and 4-dimethylaminopyridine (9.7 mg, 0.08 mmol). The mixture was allowed to 44 °C and stirred for 48 h. The mixture was partitioned between CH_2Cl_2 (40 ml) and saturated $NaHCO_3$ solution (20 ml). Extraction with CH_2Cl_2 was repeated several times. The organic layers were combined, washed with brine, dried with anhydrous Na_2SO_4, and concentrated in vacuo. The residue was chromatographed on silica gel eluting with $CHCl_3$/MeOH (15/1–6/1 v/v). The desired fraction was collected, and concentrated in vacuo to give a crude powder (23.7 mg). The powder was dissolved with small amount of MeOH, and the solution was applied on Sephadex LH-20 column (110 ml). After the column was developed with MeOH, the main fraction of elution was collected, and concentrated in vacuo to give a purple powder. The powder is dissolved in MeOH (10 ml), acidified with 0.01N HCl solution, and stirred until its color changed to yellow. The solution was concentrated in vacuo to dryness, the residue was treated with Et_2O (10 ml), and then filtrated. The precipitate was washed with diethyl ether, and dried in vacuo to give **4** (18.6 mg, 31%) as a yellow powder (purity was 97%); ^{1}H NMR (CD_3OD δ (ppm) from TMS as an interval standard): δ 1.30 (m, 2H), 1.40–1.70 (m, 5H), 2.10 (t, J = 7.4 Hz, 2H), 2.55 (t, J = 6.5 Hz, 2H), 2.60 (d, J = 12.8 Hz, 2H), 2.83 (dd, J = 12.8, 5.2 Hz, 2H), 3.08 (m, 1H), 3.41 (t, J = 13.2 Hz, 2H), 4.22 (m, 1H), 4.42 (m, 1H), 4.93 (s, 3H), 6.26 (s, 2H), 7.52 (s, 1H), 8.10 (d, J = 9.0 Hz, 1H), 8.13 (s, 1H), 8.15 (d, J = 9.0 Hz, 1H), 8.34 (d, J = 9.0 Hz, 1H), 8.57 (d, J = 9.0 Hz, 1H), 9.96 (s, 1H); ^{13}C NMR (CD_3OD δ (ppm) from TMS as an interval standard): δ 26.8, 29.4, 29.7, 35.2, 36.3, 36.6, 41.0, 52.6, 56.9, 61.6, 63.3, 64.2, 69.5, 104.3, 105.1, 107.0, 114.9, 116.9, 119.6, 121.8, 127.0, 127.1, 129.9, 132.3, 133.2, 134.2, 146.6, 148.2, 150.6, 150.8, 151.8, 166.0, 176.1, and 176.9; FAB-MS m/z 661 (M^+, $C_{34}H_{37}N_4O_8S$) (Scheme 1).

2.2. Construction of T7 phage library from human leukocytes

*Hin*dIII random primer (dTTNNNN), MMLV-RT, methylation dNTP, *Escherichia coli* DNA pol I, T4 DNA polymerase and *Eco*RI/*Hin*dIII linker were purchased from Novagen (Madison, WI). The T7 phage library alternating peptide sequence was made as follows. Total RNA was extracted from human leukocytes using the RNeasy Maxi kit (Qiagen, Amsterdam, The Netherlands) and 400 μg was then applied to oligotex-dT30 resin (Takara, Tokyo, Japan) to obtain purified poly $(A)^+$ mRNA. An aliquot (4 μg) of poly $(A)^+$ mRNA was primed with *Hin*dIII random primer (dTTNNNN), and first strand cDNA was synthesized with MMLV-RT using methylated dNTPs. Second strand cDNA was synthesized with *E. coli* DNA polymerase I. The ends of the double stranded cDNA product were then made flush with T4 DNA polymerase. The flushed double stranded cDNA was ligated with *Eco*RI/*Hin*dIII linker and then digested with *Eco*RI and *Hin*dIII. The cDNA was inserted into the *Eco*RI/*Hin*dIII site of T7 phage 10-3b vector and packaged. The titer of the primary recombinants was 4×10^6 pfu/ml.

2.3. Panning the phage library

A modified version of the panning technique given in the manufacturer's instructions (Novagen) was used in this study. Biotinylated NK109 (**4**; 100 pmol) was immobilized into 4 wells of an avidin coated 96 well plate after dilution

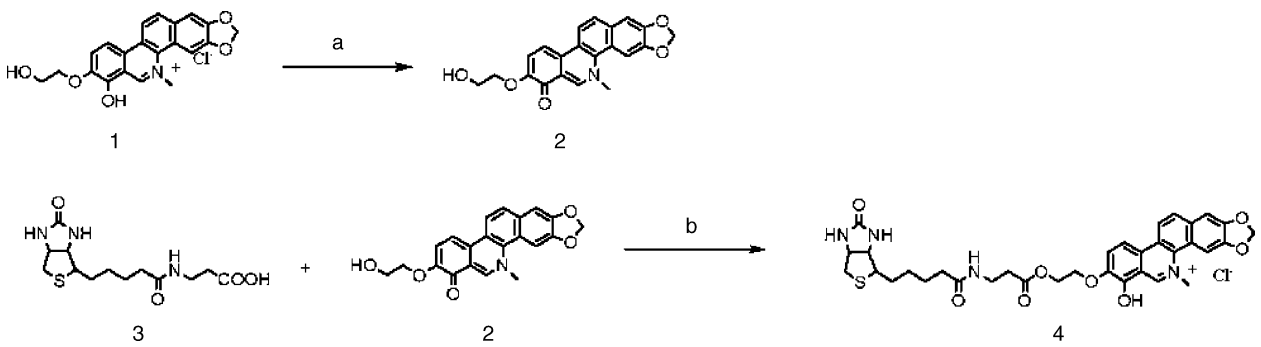

Scheme 1. Synthesis of **4**. Reagent: (a) NaOH, H_2O–CH_2Cl_2; (b) (i) DCC, DMAP, CH_2Cl_2 and (ii) HCl, MeOH.

in 200 μl of TBD buffer (50 mM Tris–HCl, pH 8.0, 10% DMSO). The solution was incubated for 1 h at room temperature. After washing each well in TBD buffer, 200 μl of TBD buffer containing 3% skimmed milk was added into each well and incubated for 1 h at room temperature for blocking. The blocking solution was discarded and 100 μl of T7 phage library (approximately 2×10^9 pfu) or 200 μl of amplified phage library (approximately 1×10^{10} pfu) was added. After 1 h incubation at room temperature the phage solution was removed and the wells were washed 10 times with 200 μl of TBD buffer. Bound phage was selectively removed by adding 100 μl of TBD buffer containing 10 nmol of free NK109. After 30 min incubation at room temperature the solution was recovered. The eluted phage was then applied to the host cells (*E. coli* BLT5615). The titer was monitored at each panning step. Blank wells, without immobilized NK109, were prepared and the eluted phage titers were compared to those of the binding phage. The eluted phage solution at each step was used for the immediate infection of 2 ml *E. coli* BLT5615. Incubation with shaking at 37 °C was continued until lysis was observed. Amplified phage titers of each panning round were estimated as approximately 10^{11} pfu/ml.

2.4. Validation of interaction between monoclonal T7 phage and ligand by reverse affinity assay

The T7 phage mixture from the final round of panning was incubated at low density on an LB plate containing 50 μg/ml of carbenicillin. Individual plaques were randomly picked and diluted into 50 μl of phage extraction buffer (20 mM Tris–HCl pH 8.0, 100 mM NaCl, 6 mM $MgSO_4$). Isolated phage particles were amplified with *E. coli* BLT5615 and used for reverse affinity validation and PCR-amplification. For reverse affinity validation, 1 μl of each amplified phage solution was spotted onto freshly prepared top-agarose plates containing non-infected BLT5615 cells. After 3 h, spots appeared as a circle composed of monoclonal phage, and the areas of the circular drop were transferred onto a nitrocellulose membrane. The membrane was blocked with the blocking buffer (3% skimmed milk, 50 mM Tris–HCl pH 8.0, 150 mM NaCl, 10% DMSO) for 1 h at room temperature. After extensive washing with TBD buffer, the membrane was incubated with 3 ml of TBD buffer containing 15 nmol of biotinylated NK109 and 3 μl of alkaline phosphatase–avidin (ZYMED Laboratories Inc., San Francisco, CA) for 1 h at room temperature. The membrane was then washed three times with TBD buffer and developed in the presence of 10 ml AP buffer (100 mM Tris–HCl pH 8.8, 100 mM NaCl, 5 mM $MgCl_2$) containing 30 μl of BCIP (50 mg/ml; 5-bromo-4-chloro-3-indolyl phosphate, 4-toluidine salt in DMF) until signals appeared. The signals were scanned and quantified by NIH image software on a personal computer.

2.5. PCR amplification and sequencing

For PCR amplification of DNA fragments and sequencing, 5 μl of T7 phage solution was used as template. T7 UP new (TGCTAACTTCCAAGCGGACC) and T7 Down (AACCCCTCAAGACCCGTTA) primers, corresponding to the sequences in the phage vector DNA that flank the inserts, were used to amplify cDNA sequences. PCR was performed in a 20 μl reaction mixture with gene *Taq* polymerase (Nippon gene, Tokyo, Japan). Amplified fragments were analyzed by agarose gel (1.5%) electrophoresis and purified with MagExtractor (TOYOBO, Osaka, Japan). DNA fragments were sequenced using PRISM BigDye terminator ready reaction kit ver 3.1 (PE-ABI, Foster City, CA) and sequenced on an ABI3100 sequencer (Applied Biosystems, Foster City, CA).

2.6. Surface plasmon resonance (SPR) analysis

SPR analysis was performed on a BIAcore 3000 (Biacore AB, Uppsala, Sweden). The synthesized peptides were immobilized covalently on a hydrophilic carboxymethylated dextran matrix on a CM5 sensor chip (Biacore AB) using a standard amine coupling reaction in 10 mM CH_3COONa pH 4.0 at a level of about 200 resonance units. Pep14 (SGVMLGDPNSSRIP) and pep9 (SGVMLGDPN) were purchased from AnyGen Co. Ltd. (Puk-gu, Kwang-ju, Korea). The C2 domain of PKC was expressed in *E. coli* and purified according to a previous report [12]. For constructing the mutant form of C2 domain, PCR was carried out by using 0.2 μM of oligo nucleotides, C2P32A-S (CCCTATGGATGCAAACGGGCTTTCAG) and C2P32A-S (CTGAAAGCCCGTTTGCATCCATAGGG) from 100 ng of the plasmid inserted C2 domain of PKC (mutation points were underlined). The amplified fragment was digested with *Dpn*I for 1 h at 37 °C. The digested fragment was transformed into *E. coli*, and the mutation point of plasmid was confirmed by sequnecing. The mutant form of C2 domain was expressed in *E. coli* and purified as well as the C2 domain. The purified C2 domain, mutant form of C2 domain and synthesized peptides were immobilized covalently on a CM5 sensor chip, respectively. Binding analyses were carried out in HBS-EP buffer (10 mM HEPES pH 7.4, 150 mM NaCl, 3.4 mM EDTA, 0.005% surfactant P20) containing 8% DMSO at a flow rate of 20 μl/min. Appropriate concentrations of NK109 were injected over the flow cell. The bulk effects of DMSO were subtracted using reference surfaces. The chips were regenerated with 30 injections of 10 mM NaOH and 1 M NaCl. To derive binding constants, data was analyzed by means of global fitting using the BIAevaluation software version 3.1 (Biacore AB).

2.7. Small molecule pull-down assay

Oligonucleotides encoding the displayed amino acid sequences of selected phage were used to construct expres-

sion plasmids of GST-peptide fusion proteins. For the construction of pGSTpep10 (LGDPNSSRIP), sense strand oligonucleotide, pep10-S (GATCCATGCTCGGGGATCCGAATTCAAGCAGGATCCCTTGAG) and anti-sense strand, pep10-AS (AATTCTCAAGGGATCCTGCTTGAATTCGGATCCCCGAGCATG) were annealed and inserted into the *Bam*HI and *Eco*RI sites in pGEX 6P-1. Similarly 10 mutants of the GSTpep10 protein in which each residue was replaced with alanine (GCT in nucleotide sequence) were constructed. The expression plasmids were transformed into *E. coli* BL21(DE3) pLysS. For expression, 50 ml of LB medium containing ampicillin (50 μg/ml) and chloramphenicol (50 μg/ml) was inoculated with 500 μl of overnight culture. When the absorbance at 600 nm reached 0.6, heterologous gene expression was induced with 1 mM isopropyl-β-D-thiogalactoside for 4 h at 37 °C. The cells were then harvested and disrupted by sonication in the 2.5 ml of TBS buffer containing 1% Triton-X 100. For purification of the recombinant protein, 50 μl of glutathione sepharose 4B beads (50% slurry) was added to 2 ml of soluble protein extract. After washing three times with 1 ml of TBS buffer, recombinant protein was eluted by the addition of 30 μl of glutathione elution buffer (10 mM reduced glutathione, 50 mM Tris–HCl, pH 8.0) three times. The preparation was analyzed by SDS polyacrylamide gel electrophoresis and protein was visualized by staining the gel with Coomassie brilliant blue. For NK109 pull-down assays, 10 μl of the recombinant protein (1.5 μM) and 5 μM of biotinylated NK109 in the presence or absence of 5 μM of free NK109 in 500 μl of TBSD buffer was incubated with rotation at 4 °C overnight. Streptavidin beads (Sigma-Aldrich, St Louis, MO) were added and incubated for 30 min at room temperature. After washing three times with 1 ml of TBST (0.1% Tween-20), SDS sample buffer was added and the sample was analyzed by SDS polyacrylamide gel electrophoresis. Protein on the gel was visualized by silver staining. The stained gels were scanned using NIH image software. Raw data was normalized by the ratio of each peptide fused GST protein against monomeric avidin protein.

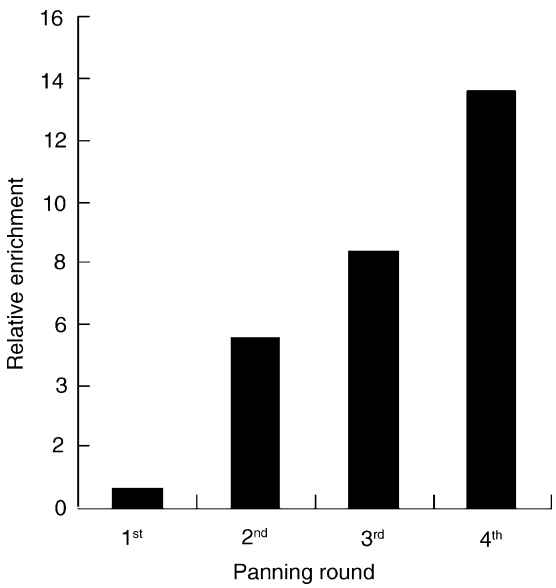

Fig. 1. Relative enrichment of phage particles binding to biotinylated NK109 (**4**). Relative enrichment was determined by the relationship between phage titer eluted from a biotinylated NK109 coated well and a non-coated well.

2.8. Modeling of NK109 complex with pep10

The structure of NK109 was prepared in CDX format using ChemDraw (CambridgeSoft, Cambridge, MA), and then converted to a three-dimensional structure and energy minimized in Chem3D (CambridgeSoft). Partial atomic charges for NK109 were computed using the PM3 Hamiltonian within MOPAC [14]. The protein module in Tinker [15] was used to generate the initial conformation of pep10. The energy minimization using the Amber94 force

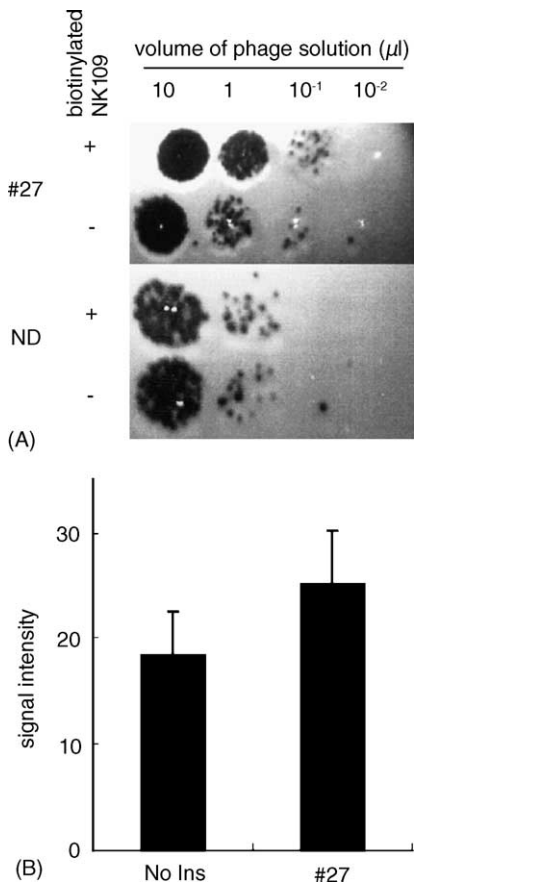

Fig. 2. Validation of an affinity for NK109 (**1**) and phage clone #27. (A) Association of NK109 (**1**) coated well to the phage clone #27. Titer of phages from a biotinylated NK109 (**4**) coated and non-coated well are indicated. Diluted phage solution spotted on an agarose plate exhibited plaques as black dots. The phage clone #27 showed significant differences, whereas the ND phage clone displayed no significant differences. (B) Reverse affinity analysis of biotinylated NK109 (**4**) and phage clone #27. No Ins, phages with no inserted DNA fragment as a negative control. Signal intensities were means from four spots. Error bar indicates standard deviations.

field [16] was performed with Tinker. During the minimization, RMSD gradient limits were 0.01.

Automated docking was carried out with the AutoDock 3.0 Lamarckian Genetic Algorithm [17] on a COMPAQ Alphastation DS20E (double 833 MHz processors and 1024 MB of memory). A binding free energy scoring function in the AutoDock was based on an empirical function derived by linear regression analysis of a large set of diverse protein–ligand complexes with known inhibition constants. There are many successful examples of structures of protein–ligand systems studied by AutoDock [18,19]. During a docking simulation in AutoDock, the receptor is rigid and fixed while the ligand is flexible and can both translate and rotate. In this study, we assumed that NK109 was rigid and pep10 was flexible for constructing the model of the NK109/pep10 complex because the initial conformation of pep10 was not considered to be the binding conformation and the NK109 had a rigid structure. Docking was performed in a 80 Å × 80 Å × 80 Å volume, with a grid spacing of 0.375 Å centered on NK109. The number of energy evaluations was set at 5×10^6. Each simulation performed a total of 100 runs. Other parameters were default values. Rotational bonds in pep10 were assigned with AutoTors [17]. All torsions, except the peptide bonds, were unconstrained during the docking. After docking had been carried out, the lowest-energy docking pose was used for analysis.

2.9. Protein kinase C inhibition assay

PKC from rat brain was purchased from Sigma-Aldrich. PKC and appropriate concentrations of NK109 in 25 mM of Tris–HCl, pH 7.5, 10% DMSO were incubated at room temperature for 5 min. After pre-incubation, 50 μl of the

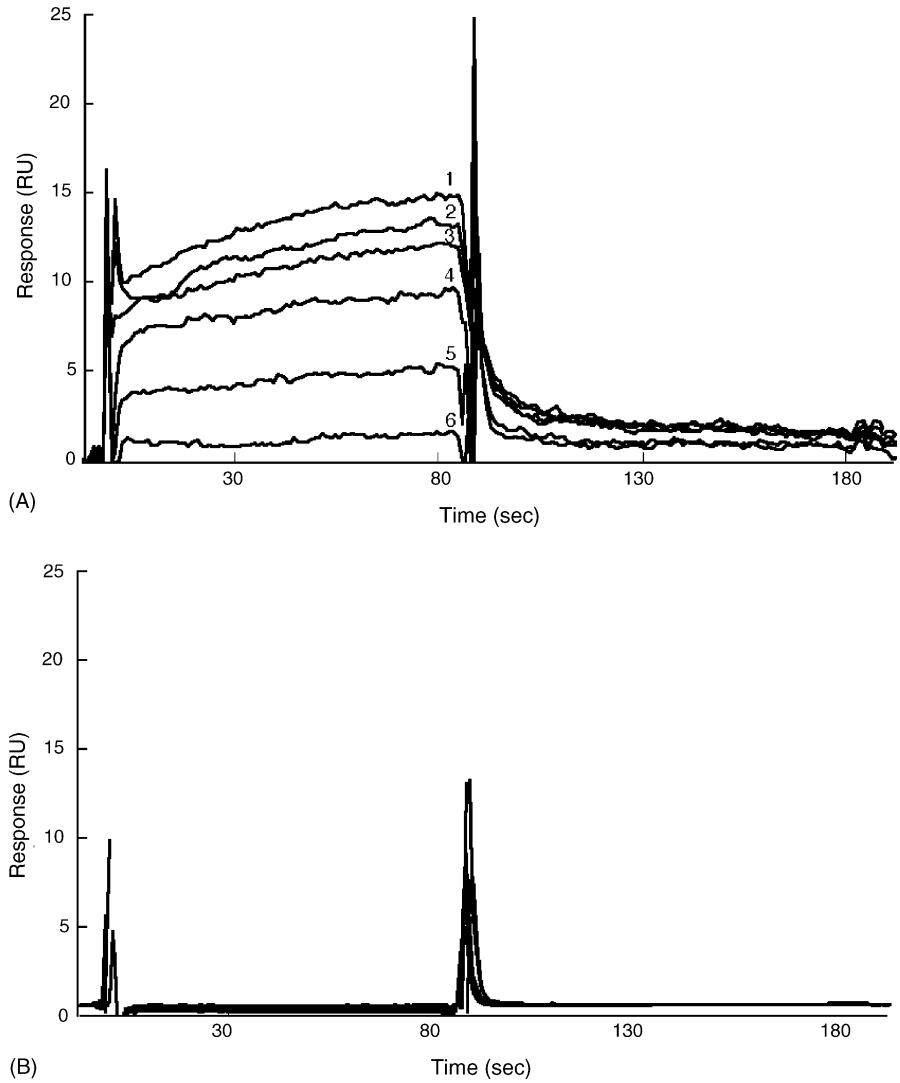

Fig. 3. Surface plasmon resonance analysis of the binding of NK109 (**1**) and pep14 (A) and pep9 (B). A representative overlay of a sensorgram generated for six different concentrations of NK109 (curve 1, 750 μM; curve 2, 700 μM; curve 3, 650 μM; curve 4, 550 μM; curve 5, 400 μM; curve 6, 200 μM) injected over flow cells on the immobilized pep14 (A). The background resulting from injection of running buffer alone was subtracted from the data before plotting. Response units (RU) were generated by subtraction of the background signal generated simultaneously on the control flow cell. For a sensorgram with the pep9 immobilized chip, all RUs measured from different concentrations of NK109 (0 μM to 750 μM) show less than 1.0.

incubation mixture containing 25 mM Tris–HCl, pH 7.5, 5 mM $MgCl_2$, 500 μg/ml of histones (Type IIIS), 25 μg/ml of 1,2-dioleoyl-*rac*-glycerol, 500 μg/ml of phosphatidyl serine, 1 mM $CaCl_2$, 10 μM ATP, [γ-^{32}P]-ATP (9.25 kBq) was added into the solution of enzyme and NK109. After incubation for 5 min, the reaction was terminated by the addition of 50 μl of 20 mM ATP. The reaction mixtures were collected on DE52 DEAE cellulose (Whatman, Clifton, NJ) and extensively washed with 75 mM phosphate. The radioactivity was normalized for non-specific activity by assaying in the absence of 1,2-dioleoyl-*rac*-glycerol, phosphatidyl serine and $CaCl_2$.

3. Results

3.1. Selection of the T7 phage associated with NK109

Peptides derived from human leukocytes were analyzed for their ability to bind NK109 by employing a biopanning technique. A T7 phage library displaying a library of peptides was screened by affinity selection using NK109 as bait. Phage particles displaying affinity for biotinylated NK109 were efficiently enriched during the panning procedure (Fig. 1). It was expected that the eluted phage at the fourth round of panning would include those having a high affinity for NK109. We confirmed the affinity for immobilized NK109 by using single phage clones. The 36 phage clones were randomly selected and amplified. Among the 36 phage clones, the titer of phage clone #27 during elution from the well containing immobilized NK109 indicated significant binding compared with the blank well (Fig. 2A). Next, we validated NK109 affinity of the phage clone #27 by using reverse affinity analysis. The ratio of affinities between the immobilized phage and mobilizing biotinylated NK109 was measured. The phage clone #27 showed a higher affinity ratio than one inserted no fragment (Fig. 2B). These results suggested that phage clone #27 had a high affinity for NK109.

3.2. The peptide, LGDPNSSRIP, interacts with NK109

The inserted cDNA of phage clone #27 was frame-shifted, resulting in a peptide of five amino acids, S-S-R-I-P. To identify amino acids required for affinity against NK109, we performed surface plasmon resonance analysis with two peptides, pep14 and pep9. Pep14 consisted of fourteen amino acids (SGVMLGDPNSSRIP), including nine (SGVMLGDPN) from the capsid protein of T7 phage in addition to five (SSRIP) from the inserted cDNA. Pep9 consisted of only the nine amino acids from the capsid protein. These peptides were immobilized on a sensor chip and NK109 was injected. The sensorgrams of pep14 were clearly dose-dependent with the concentration of NK109, whereas those for pep9 were not (Fig. 3). An equilibrium dissociation constant (K_D) between pep14 and NK109 was determined to be 980 μM. To confirm the interaction between the peptide and NK109, we performed a small molecule pull-down assay. In this method, small molecule associated proteins are co-precipitated with avidin beads using biotinylated derivatives. The LGDPNSSRIP peptide fused GST protein, GST-pep10, was expressed in *E. coli* and purified. As shown in Fig. 4A, a significant amount of GST-pep10 protein was co-precipitated with avidin beads via biotinylated NK109. The association was disrupted by the addition of NK109 as a competitor. These results suggest a specific association between NK109 and the LGDPNSSRIP peptide.

3.3. Target motif of NK109 is PNxxxxP

In order to identify the residues required for interaction with NK109, we performed binding analysis using mutants of the LGDPNSSRIP peptide in which each amino acid was successively replaced with alanine in the GST fused protein. The mutant peptides fused to GST protein were named GST-L1A, -G2A, -D3A, -P4A, -N5A, -S6A, -S7A, -R8A, -I9A, and -P10A. The mutants P4A, N5A and P10A displayed a drastic reduction in affinity for NK109, while mutants S7A and R8A had a slightly lower affinity (Fig. 5).

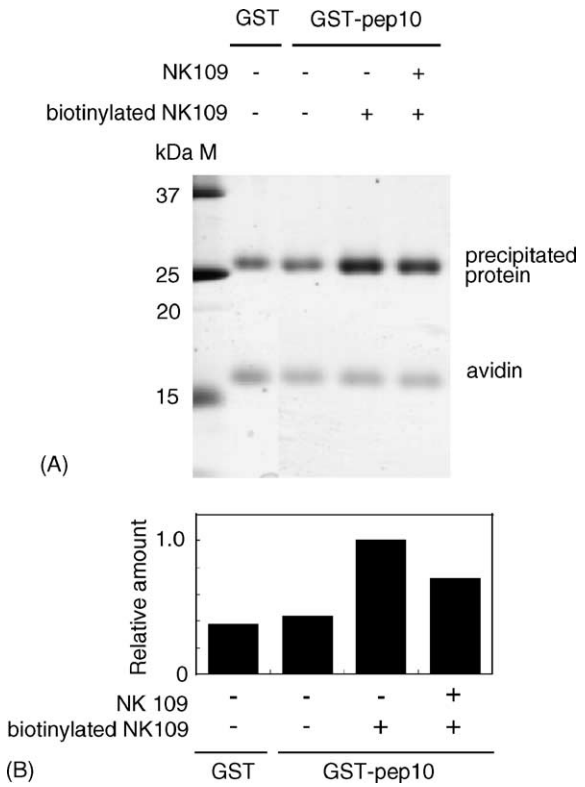

Fig. 4. Small molecule pull-down assay with NK109 and GST fused peptides. (A) Silver staining of SDS polyacrylamide gel. Incubated avidin beads with GST or GST-pep10 protein in the presence (+) or absence (−) of NK109 (5 nmol) were loaded. Molecular marker was loaded on a lane M. Monomeric avidins were visible at approximately 16 kDa. (B) The relative amount of GST and GST fused peptides in panel A were normalized with the amount of monomeric avidin in the same lane. Results are given in the form of a bar graph.

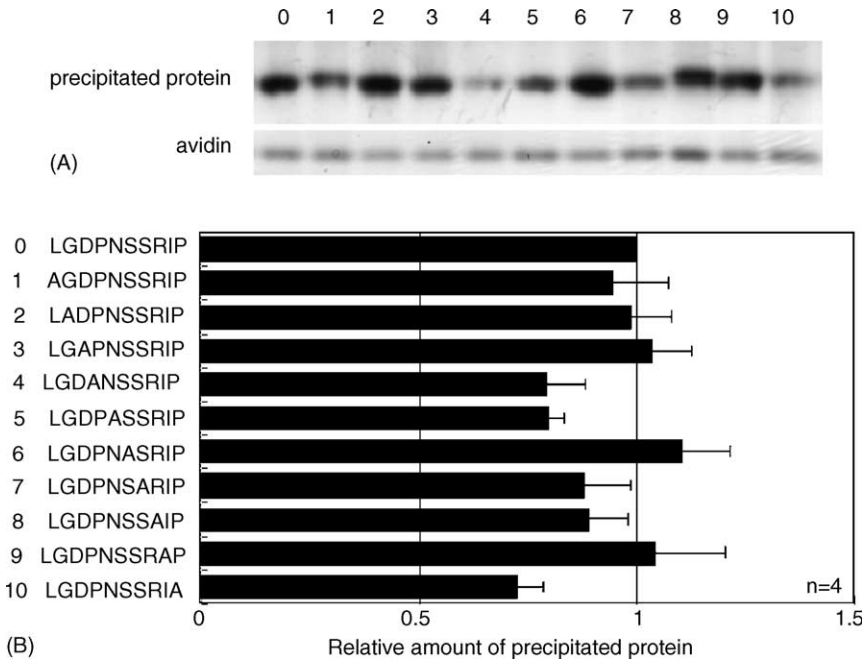

Fig. 5. Alanine scans of the LGDPNSSRIP peptide. Eleven peptides (GST-L1A, -G2A, -D3A, -P4A, -N5A, -S6A, -S7A, -R8A, -I9A, and -P10A) corresponding to the pep10 sequence but with the systematic replacement of each residue with alanine were expressed as GST fusion proteins. (A) A silver staining of SDS polyacrylamide gel among independent four experiments: lane 0, GST-pep10; lane 1, GST-L1A; lane 2, GST-G2A; lane 3, GST-D3A; lane 4, GST-P4A; lane 5, GST-N5A; lane 6, GST-S6A; lane 7, GST-S7A; lane 8, GST-R8A; lane 9, GST-I9A; lane 10, GST-P10A. (B) The relative amount of GST fused peptides in panel A were normalized with the amount of monomeric avidin in same lane. Results are given in the form of a bar graph.

Mutants L1A, G2A and D3A had the same binding properties as the original peptide. These results indicate that the seven residues from P4 to P10 were required for the molecular recognition of NK109. Moreover, the three residues P4, N5 and P10 are the most important for this interaction. To predict the binding structure of NK109 with the peptide LGDPNSSRIP, we carried out in silico simulation with docking studies and molecular dynamics. The predicted binding structure clearly shows the importance of the side chains of three residues, P4, N5 and P10, for the affinity (Fig. 6). We, therefore, propose that the target motif of NK109 is PNxxxxP, where x represents any amino acid residue.

3.4. NK109 inhibits PKCα via the C2 domain, including PNxxxxP motif

Chelerythrine, a derivative of benzo[*c*]phenanthridine is a specific protein kinase C inhibitor [6]. Thus, we searched whether PKC has the PNxxxxP motif. Indeed, PKCα shows the PNGLSDP sequence in the C2 domain, which includes Ca^{2+} binding region conserved among classical PKCs (Fig. 7A) [13]. To confirm an interaction between NK109 and the C2 domain, we carried out SPR analysis with the recombinant C2 domain from PKCα and NK109. The sensorgrams were clearly dose-dependent with the concentration of NK109 (Fig. 7B). The K_D value between the C2 domain and NK109 was determined to be 24 μM. In order to confirm the significance of PNxxxxP motif in C2 domain for the NK109 interaction, we also performed SPR analysis with the mutant protein of C2 domain, which was disrupted a PNxxxxP motif by amino acid substitution of the first Pro to Ala (PNGLSDP to ANGLSDP). Fig. 7C shows the mutant form of C2 domain apparently decreased the interaction with NK109. The K_D value of the mutant form of C2 domain is 3.2 mM. These indicate that PNxxxxP of C2 domain is required for the NK109 interaction. Next, we measured the inhibitory activity of NK109 against PKC kinase activity to verify a functional association between NK109 and the C2 domain. Fig. 7D clearly shows the inhibition dose-dependent curves of NK109 against PKC. The IC_{50} value was estimated to be 73 μM. These results demonstrate that NK109 inhibits the kinase activity of PKC by interacting with the C2 domain of PKC. We, therefore, conclude that the target motif for NK109 is PNxxxxP.

4. Discussion

In this report we describe the isolation a phage displaying the LGDPNSSRIP peptide that has an affinity for NK109. As shown Fig. 5, the proline residues Pro4 and Pro10 and asparagine Asn5 in the amino acid sequence of the displayed peptide were required for good association with NK109. Serine (Ser7) and arginine (Arg8) were also important. Moreover, docking structures predicted from molecular dynamic calculations indicate that the side chains of Pro4, Pro10 and Asn5 hold NK109 in an orientation akin to that of the forefinger and thumb. It is likely that

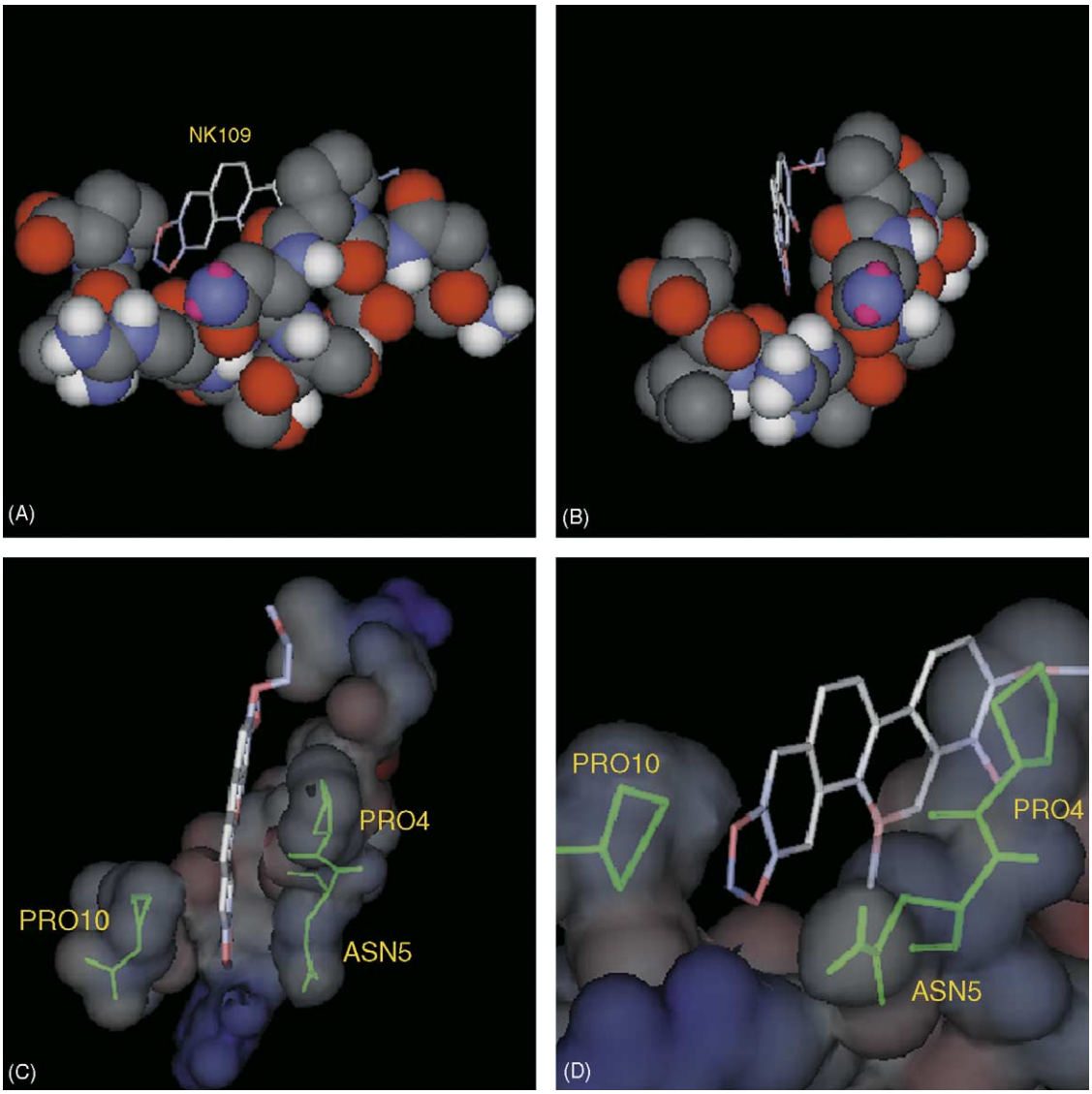

Fig. 6. Docking simulation with molecular dynamics of NK109 (**1**) and the pep10. (A) Interaction between NK109 and pep10. (B and C) Different angles from panel A. (D) Magnification of docking site.

amino acids Ser6 to Ile9 form a palm-like structure for stabilization of the NK109–peptide complex. The side chains of Ser7 and Arg8 might enhance the stability of the complex by increasing the hydrophilic nature of the interaction. It is noteworthy that the two proline residues stack with the polycyclic portion of NK109, rather than bending the polypeptide chain (Fig. 6C and D). Taken together these results suggest that NK109 binds to the PNxxxxP motif. Indeed, NK109 inhibits the activity of PKC, which has a PNxxxxP motif (PNGLSDP) in the C2 domain [20,13]. The PNGLSDP sequence is located within the Ca^{2+} binding region of the C2 domain, indicating that NK109 might inhibit PKC by interfering with the association between Ca^{2+} and the enzyme.

NK109 is an anti-tumor drug and has various effects on several different cell lines. Previous reports indicated that NK109 inhibits DNA topoisomerase II activity by stabilizing the cleavable complex [2,21]. The amino acid sequence of topoisomerase II alpha does not contain a PNxxxxP motif. However, interestingly, topoisomerase II beta does contain a PNxxxxP motif at the carboxyl terminus, indicating a possible interaction with NK109. This means NK109 inhibits both topoisomerase II and PKCα. Because proline residues generally break the tertiary structure, the PNxxxxP region is likely to form an independent structural unit within the overall protein structure. Therefore, NK109 can easily interact with the PNxxxxP motif of various proteins to influence a number of protein functions.

The amount of NK109 required for inhibition of DNA topoisomerase II activity is >100 μM [1,2] and of PKCα is 73 μM. Since IC_{50} value of NK109 in the cell lines is submicromolar, unknown target protein(s) clearly exist in the cell. We revealed here NK109 associated the PNSSRIP sequence. This suggests that proteins containing a sequence with good homology to PNSSRIP would be predicted to bind NK109 with higher affinity than topoi-

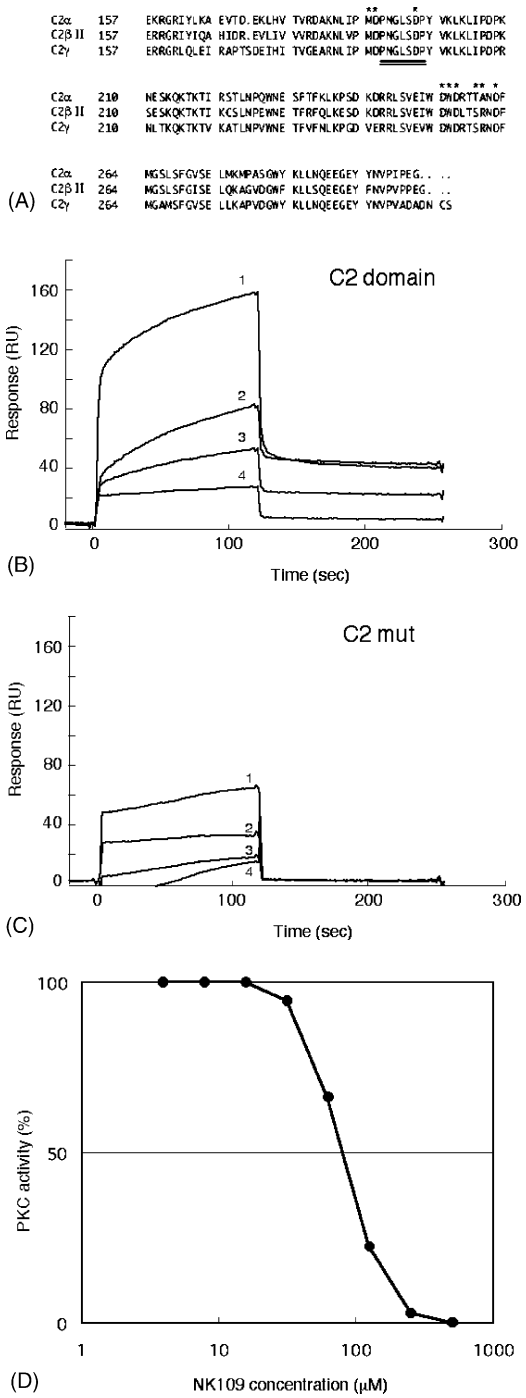

Fig. 7. (A) Amino acid sequence alignment of the C2 domains of PKCα, PKCβII and PKCγ. The coordinating-calcium residues of the C2 domains of PKCα crystal structure are indicated by asterisks. Double-underline shows PNxxxxP motif in the C2 domain. (B and C) Surface plasmon resonance analysis of the binding of NK109 and C2 domain (B) and mutant form of C2 domain (C) from PKCα. Four different concentrations of NK109 (**1**) (curve 1, 50 μM; curve 2, 12.5 μM; curve 3, 6.25 μM; curve 4, 3.125 μM) were injected over a flow cell on the immobilized C2 domain of PKCα. The background resulting from injection of running buffer alone was subtracted from the data before plotting. (D) Dose–response curves of NK109 to PKC kinase activity. The PKC used at 0.05 units. The PKC kinase activities were measured as described in the text. The PKC kinase activity in the presence or absence of $CaCl_2$, DG and PS is represented as 100 or 0%, respectively.

somerase II and PKCα. Thus, next step for elucidating the anti-cancer mechanism of NK109 is identification of a main target. We are now studying several candidates of a main target of NK109.

Acknowledgment

This work was supported by Nippon Kayaku Co. Ltd. and funded partially from JSPS.

References

[1] Kabasawa T, Kobayashi F, Ekimoto H, Suzuki M, Hanaoka M. A novel benzo[c]phenanthridine derivative, NK109, is a highly active anticancer agent and DNA topoisomerase II inhibitor. Proc Am Assoc Cancer Res 1996;37:427.

[2] Kanzawa F, Nishio K, Ishida T, Fukuda M, Kurokawa H, Fukumoto H, et al. Anti-tumour activities of a new benzo[c]phenanthridine agent 2, 3-(methylenedioxy)-5-methyl-7-hydroxy-8-methoxybenzo[c]phenanthridinium hydrogensulphate dihydrate (NK109), against several drug-resistant human tumour cell lines. Br J Cancer 1997;76:571–81.

[3] Nakanishi T, Suzuki M, Saimoto A, Kabasawa T. Structural considerations of NK109, an antitumor benzo[c]phenanthridine alkaloid. J Nat Prod 1999;62:864–7.

[4] Nakanishi T, Masuda A, Suwa M, Akiyama Y, Hoshino-Abe N, Suzuki M. Synthesis of derivatives of NK109, 7-OH benzo[c]phenanthridine alkaloid, and evaluation of their cytotoxicities and reduction-resistant properties. Bioorg Med Chem Lett 2000;10:2321–3.

[5] Fleury F, Sukhanova A, Ianoul A, Devy J, Kudelina I, Duval O, et al. Molecular determinants of site-specific inhibition of human DNA topoisomerase I by fagaronine and ethoxidine. J Biol Chem 2000;275:3501–9.

[6] Chmura SJ, Dolan E, Cha A, Mauceri HJ, Kufe DW, Weichselbaum RR. In vitro and in vivo activity of protein kinase C inhibitor chelerythrine chloride induces tumor cell toxicity and growth delay in vivo. Clin Cancer Res 2000;6:737–42.

[7] Rodi DJ, Janes RW, Sanganee HJ, Holton RA, Wallace BA, Makowski L. Screening of a library of phage-displayed peptides identifies human Bcl-2 as a taxol-binding protein. J Mol Biol 1999;285:197–203.

[8] Sche PP, McKenzie KM, White JD, Austin DJ. Display cloning: functional identification of natural product receptors using cDNA-phage display. Chem Biol 1999;6:707–16.

[9] Jin Y, Yu J, Yu YG. Identification of hNopp140 as a binding prtner for doxorubicin with a phage display cloning method. Chem Biol 2002;9:157–62.

[10] Yamazaki T, Aoki S, Ohta K, Hyuma S, Sakaguchi K, Sugawara F. Synthesis of an immunosuppressant SQAG9 and determination of the binding peptide by T7 phage display. Bioorg Med Chem Lett 2004;14:4343–6.

[11] Shim JS, Lee L, Park HJ, Park SJ, Kwon HJ. A new curcumin derivative, HBC, interferes with the cell cycle progression of colon cancer cells via antagonization of the Ca^{2+}/calmodulin function. Chem Biol 2004;11:1455–63.

[12] Romanov VI. Phage display selection and evaluation of cancer drug targets. Cancer Drug Targets 2003;3:119–29.

[13] Torrecillas A, Corbalán-García S, Gómez-Fernández JC. Structural study of the C2 domains of the classical PKC isoenzymes using infrared spectroscopy and two-dimensional infrared correlation spectroscopy. Biochemistry 2003;42:11669–81.

[14] Cornell WD, Cieplak P, Bayly CI, Gould IR, Merz KM, Ferguson Jr DM, et al. A second generation force field for the simulation of proteins, nucleic acids, and organic molecules. J Am Chem Soc 1995;117:5179–97.

[15] Ponder JW, Richards FM. An efficient newton-like method for molecular mechanics energy minimization of large molecules. J Comput Chem 1987;8:1016–24.
[16] Stewart JJ. MOPAC: a semiempirical molecular orbital program. J Comput Aided Mol Des 1990;4:1–45.
[17] Morris GM, Goodsell DS, Halliday RS, Huey R, Hart WE, Belew RK, et al. Automated docking using a lamarckian genetic algorithm and and empirical binding free energy function. J Comput Chem 1998;19:1639–62.
[18] Jenkins JL, Shapiro R. Identification of small-molecule inhibitors of human angiogenin and characterization of their binding interactions guided by computational docking. Biochemistry 2003;42:6674–87.
[19] Bartolucci C, Perola E, Pilger C, Fels G, Lamba D. Three-dimensional structure of a complex of galanthamine (Nivalin®) with acetylcholinesterase from Torpedo californica: implications for the design of new anti-Alzheimer drugs. Proteins struct function genetics 2001;42:182–91.
[20] Verdaguer N, Corbalán-García S, Ochoa WF, Fita I, Gómez-Fernández JC. Ca^{2+} bridges the C2 membrane-binding domain of protein kinase Cα directly to phosphatidylserine. EMBO J 1999;18:6329–38.
[21] Fukuda M, Inomata M, Nishio K, Fukuoka K, Kanzawa F, Arioka H, et al. A topoisomerase II inhibitor, NK109, induces DNA single- and double-strand breaks and apoptosis. Jpn J Cancer Res 1996;87:1086–91.